Cell Death and Differentiation (2016) 23, 291–302

www.nature.com/cdd

Loss of *Drosophila* i-AAA protease, dYME1L, causes abnormal mitochondria and apoptotic degeneration

Y Qi[1], H Liu[2], MP Daniels[1], G Zhang[3] and H Xu*[,1]

Mitochondrial AAA (ATPases Associated with diverse cellular Activities) proteases i-AAA (intermembrane space-AAA) and m-AAA (matrix-AAA) are closely related and have major roles in inner membrane protein homeostasis. Mutations of m-AAA proteases are associated with neuromuscular disorders in humans. However, the role of i-AAA in metazoans is poorly understood. We generated a deletion affecting *Drosophila* i-AAA, *dYME1L* (*dYME1L*^{del}). Mutant flies exhibited premature aging, progressive locomotor deficiency and neurodegeneration that resemble some key features of m-AAA diseases. *dYME1L*^{del} flies displayed elevated mitochondrial unfolded protein stress and irregular cristae. Aged *dYME1L*^{del} flies had reduced complex I (NADH/ubiquinone oxidoreductase) activity, increased level of reactive oxygen species (ROS), severely disorganized mitochondrial membranes and increased apoptosis. Furthermore, inhibiting apoptosis by targeting dOmi (*Drosophila* Htra2/Omi) or DIAP1, or reducing ROS accumulation suppressed retinal degeneration. Our results suggest that i-AAA is essential for removing unfolded proteins and maintaining mitochondrial membrane architecture. Loss of i-AAA leads to the accumulation of oxidative damage and progressive deterioration of membrane integrity, which might contribute to apoptosis upon the release of proapoptotic molecules such as dOmi. Containing ROS level could be a potential strategy to manage mitochondrial AAA protease deficiency.
Cell Death and Differentiation (2016) **23,** 291–302; doi:10.1038/cdd.2015.94; published online 10 July 2015

Mitochondria dictate the survival and well being of the eukaryotic cells, but their unique genetic system and complex biophysical characteristics make for great challenges in maintaining organelle integrity and function.[1] One challenge is ensuring the proper assembly of the protein complexes carrying out mitochondrial functions. Most mitochondrial proteins are encoded by the nuclear genome and imported into the mitochondria after synthesis.[2] However, mitochondria also contain their own genome, which encodes the core components of the electron transport chain (ETC). The mitochondrion-encoded subunits of the ETC assemble on the inner mitochondrial membrane (IMM) with the nuclear-encoded ones. Unassembled polypeptides have to be removed to maintain the stoichiometry of the ETC complexes. Another challenge is the production of reactive oxygen species (ROS), the unavoidable by-products of electron transfer, which are generated mainly at complex I (NADH/ubiquinone oxidoreductase) and complex III (ubiquinol-cytochrome *c* oxidoreductase) in the ETC.[3] Excessive ROS can damage proteins and impair mitochondrial functions.

An elaborate system of chaperones and proteases has evolved to ensure mitochondrial proteostasis.[4] The proteases are located in different submitochondrial compartments and carry out critical steps of mitochondrial biogenesis and turnover, including processing, assembly and degradation of mitochondrial proteins. Mitochondrial proteases of the AAA class (ATPases Associated with diverse cellular Activities) are the main regulators of proteostasis on the IMM,[5] which houses many important complexes including those of the ETC. The catalytic domains of AAA proteases face either the matrix (mitochondrial m-AAA proteases) or the intermembrane space (IMS) (mitochondrial i-AAA protease).[6] Despite their different topologies, mitochondrial m-AAA proteases and i-AAA protease share highly conserved protein structures and catalytic mechanism, and even an overlapping substrate specificity.[7] Mutations in the mitochondrial m-AAA proteases are responsible for neurodegenerative disorders including hereditary spastic paraplegia (HSP), spinocerebellar ataxia (SCA28) and spastic ataxia neuropathy syndrome.[8–10] However, the degenerative mechanisms remain elusive,[11] and the presence of multiple mitochondrial m-AAA proteases with redundant functions in eukaryotes complicates their analysis in animal models. By contrast, only one mitochondrial i-AAA protease has been identified in eukaryotic genomes. It coordinates mitochondrial fusion and fission,[12] and couples the mitochondrial dynamics to oxidative phosphorylation.[13] Knocking down mitochondrial i-AAA protease in cultured cells perturbed mitochondrial morphology and sensitized cells to oxidative stress and apoptotic stimuli.[14–16] However, the pathophysiological consequences of i-AAA loss of function at the animal level have been largely unknown. Yet, the absence of gene redundancy makes mitochondrial i-AAA protease particularly suitable for genetic studies exploring the function of mitochondrial AAA proteases in animal models.

[1]Laboratory of Molecular Genetics, National Heart, Lung and Blood Institute, National Institutes of Health, Bethesda, MD, USA; [2]National Cancer Institute, National Institutes of Health, Bethesda, MD, USA and [3]National Institute of Biomedical Imaging and Bioengineering, National Institutes of Health, Bethesda, MD, USA
*Corresponding author: H Xu, Laboratory of Molecular Genetics, National Heart, Lung and Blood Institute, National Institutes of Health, 10 Center Drive, Building 10, 6C212, Bethesda, MD 20892, USA. Tel/Fax: +1 301 594 5940; E-mail: hong.xu@nih.gov
Abbreviations: ETC, electron transport chain; IMM, inner mitochondrial membrane; IMS, intermembrane space; ROS, reactive oxygen species; AAA, ATPases Associated with diverse cellular Activities; IFM, indirect flight muscle; NAC, *N*-acetyl cysteine; UPR^{mt}, mitochondrial unfolded protein response; UPR^{ER}, ER unfolded protein response
Received 05.9.14; revised 30.5.15; accepted 05.6.15; Edited by E Baehrecke; published online 10.7.15

Drosophila melanogaster has been widely used to understand the biochemical processes underlying a variety of human diseases,[17] including many mitochondrial disorders such as Parkinson's disease.[18–20] In these studies, some key phenotypes of mitochondrial diseases, such as impaired locomotor activities and neural and muscular degeneration, have been successfully recapitulated in *Drosophila*. Here we demonstrate that loss of mitochondrial i-AAA protease (dYME1L) in *Drosophila melanogaster* perturbs mitochondrial proteostasis, causes mitochondrial anomalies and triggers apoptotic degeneration in neurons and muscles.

Results

***CG3499* encodes the *Drosophila* homolog of the human i-AAA protease YME1L.** Based on sequence analysis, *CG3499* is the *Drosophila* homolog of human i-AAA protease YME1L.[21] It is predicted to have a single transmembrane domain followed by an ATPase domain and an M41 peptidase domain, both of which are highly conserved among mitochondrial AAA proteases, and with human YME1L. To determine whether the CG3499 protein localizes to the mitochondria, we built a CG3499-GFP fusion protein and coexpressed it with Tom20-mCherry, a fluorescent mitochondrial marker, in *Drosophila* Schneider 2 (S2) cells. Confocal microscopic analysis showed overlapping fluorescent signals for GFP and Tom20-mCherry (Figure 1a), confirming that CG3499 (dYME1L) is a mitochondrial protein.

To obtain a *dYME1L* mutant, we mobilized the P element inserted in the first intron of *CG3499* (BL14902: KG01861). We recovered an imprecise excision with a 2 kb deletion ($dYME1L^{del}$), which removed the majority of the *dYME1L* coding region (Figure 1b). $dYME1L^{del}$ flies were homozygous-viable, but male-sterile. Compared with the wild-type flies (w^{1118}), $dYME1L^{del}$ flies had a markedly shortened lifespan (Figure 2c). The lifespan was even shorter for the homozygous mutant progeny of homozygous mothers ($dYME1L^{del}/dYME1L^{del}$) compared with that for the homozygous progeny of heterozygous mothers ($dYME1L^{del}/CyO$) (Supplementary Figure S1), suggesting a maternal effect consistent with the maternal inheritance of mitochondria. Although most maternal effects are manifested during embryonic development,[22–24] this mitochondrial mutation has a cumulative effect that extends to adulthood.

***dYME1L*^{del} causes neuronal degeneration and abnormal crista structure.** Mitochondrial mutations afflict most severely the highly energy-demanding tissues such as the nervous system and the muscles. Thus, we examined whether $dYME1L^{del}$ caused any neuronal or muscular deficiencies, using locomotor assays. Young $dYME1L^{del}$ flies appeared similar to the age-matched wild-type flies in the climbing test and the bang sensitivity assay. However, they gradually lost their climbing ability (Figure 2a), and became increasingly susceptible to seizure following mechanical stress as they aged (Figure 2b).

The progressive loss of motor control and the increased sensitivity to mechanical stress suggested defects in the muscles, the nervous system or both. To assay whether $dYME1L^{del}$ caused neurodegeneration, we examined the morphology of the adult eye, a widely used model for various human neurodegenerative diseases,[25] using electron microscopic imaging and optical neutralization techniques. $dYME1L^{del}$ flies had the full complement of ommatidium components at a young age but gradually lost rhabdomeres with age (Figure 2d and Supplementary Figure S2d), indicating an age-dependent degeneration of photoreceptor neurons. Ubiquitous expression of the *dYME1L* cDNA in the mutant background rescued most $dYME1L^{del}$ phenotypes, including shortened lifespan (Figure 2c), age-dependent locomotor impairments (Figures 2a and b) and neurodegeneration (Figure 2d and Supplementary Figure S2e). These results demonstrate that the *dYME1L* mutation is responsible for the observed neuronal, muscular and behavior defects in $dYME1L^{del}$ flies. Of note, expressing human *YME1L* also rescued these

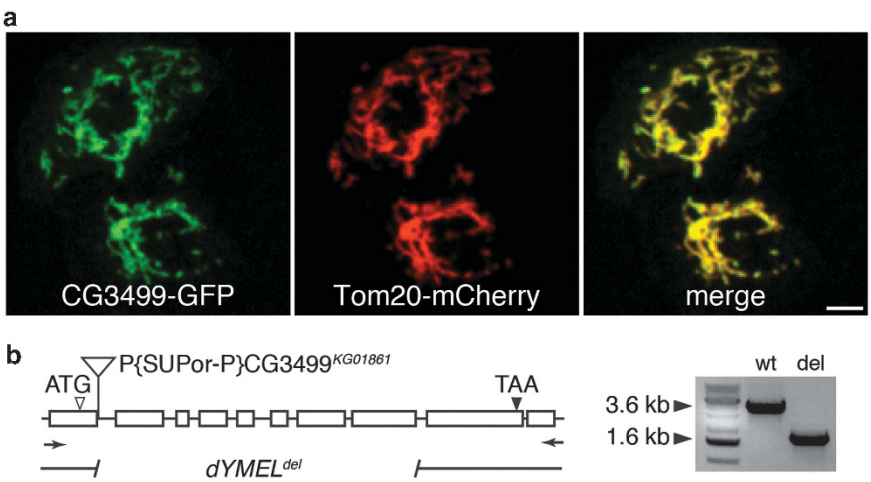

Figure 1 Generating mitochondrial i-AAA protease mutant in *Drosophila melanogaster*. (**a**) Coexpression of CG3499-GFP and Tom20-mCherry in *Drosophila* S2 cells showing their colocalization to the mitochondria. Scale bar, 5 μm. (**b**) A schematic illustration of the genomic region of *CG3499* and the CG3499-deletion allele ($dYME1L^{del}$). DNA gel electrophoresis shows a 3.6 kb fragment amplified from wild-type genomic DNA (wt) but a 1.6 kb fragment amplified from $dYME1L^{del}$ genomic DNA (del)

phenotypes (Figure 2 and Supplementary Figure S2e), confirming that CG3499 is indeed the *Drosophila* ortholog of the human mitochondrial i-AAA protease.

We further examined mitochondrial ultrastructure in the indirect flight muscle (IFM) by transmission electron microscopy (Figure 3). Compared with the wild-type mitochondria

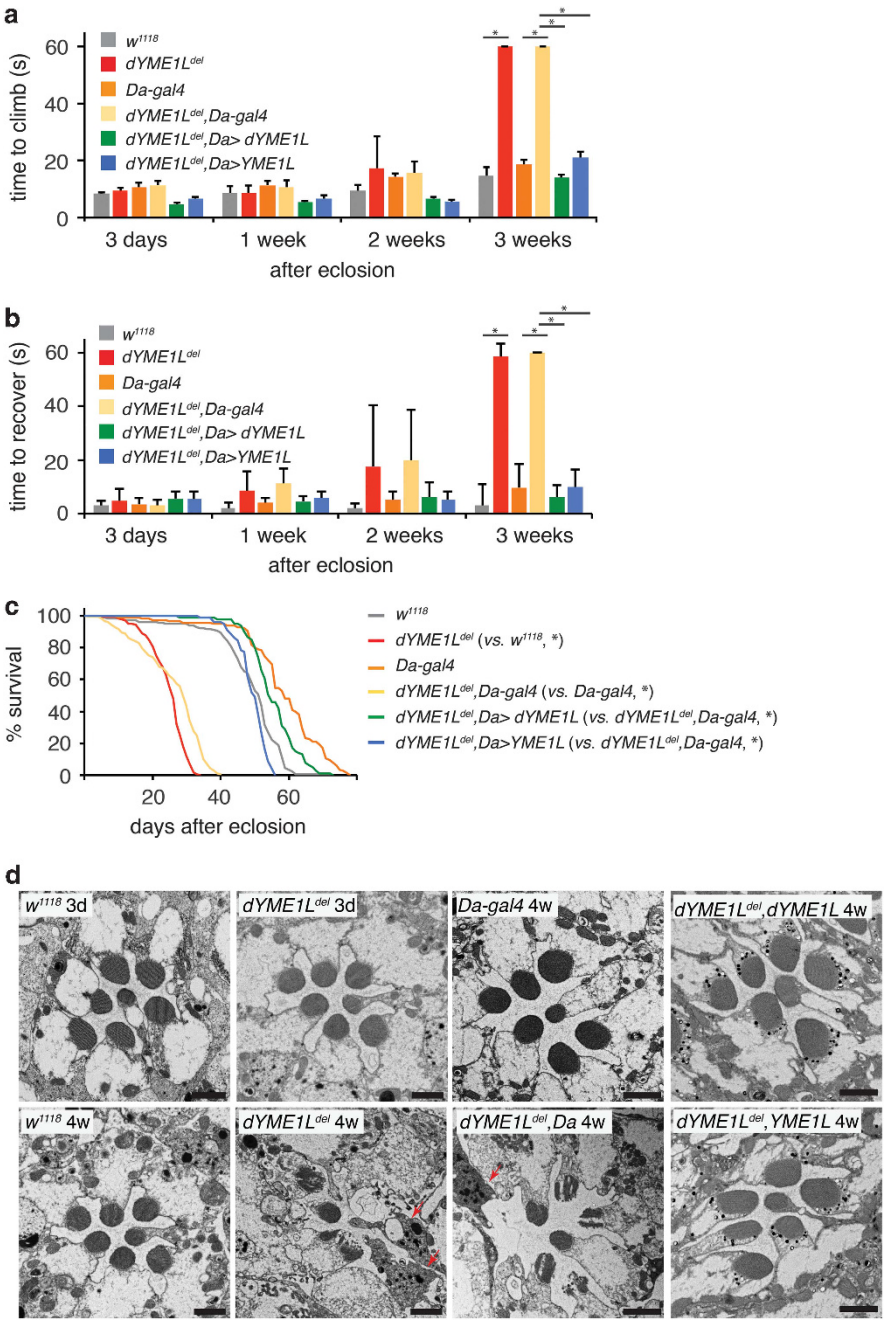

Figure 2 Phenotypic characterization of *dYME1L*^{del} flies. (**a**) *dYME1L*^{del} flies show an age-dependent locomotor impairment in the climbing tests. Expressing *dYME1L* or human homolog *YME1L* restores the climbing ability in *dYME1L*^{del} flies. Each data point represents the average of three groups of 10 flies. (**b**) *dYME1L*^{del} flies show an age-dependent decrease in the resistance to mechanical stress, which can be rescued by *dYME1L* or *YME1L* expression. Each data point represents the average of 10 individual flies. Student's *t*-test is performed between the individual genetic manipulation and its corresponding control for (**a** and **b**): *dYME1L*^{del} versus w^{1118}. *dYME1L*^{del}, *Da-gal4* versus *Da-gal4*. *dYME1L*^{del}, *Da-gal4*> *dYME1L* versus *dYME1L*^{del}, *Da-gal4* and *dYME1L*^{del}, *Da-gal4*> *YME1L* versus *dYME1L*^{del}, *Da-gal4*. *$P<0.01$ (**c**) *dYME1L*^{del} flies are short-lived and their lifespan can be rescued by the expression of either *dYME1L* or *YME1L* transgene. Log-rank test is performed between the individual genetic manipulation and its corresponding control, as indicated within parentheses after the abbreviated genotype. *$P<0.0001$. (**d**) Representative electron microscopic images from different genotypes at 3 days (3d) and 4 weeks (4w) after eclosion showing retinal degeneration in *dYME1L*^{del} flies. The red arrows indicate dying photoreceptor cells featured with signs for apoptosis: large electron-dense area in the nucleus for condensed chromatin, cell blebs and shrinkage, cytoplasmic condensation and losing cell–cell contacts with neighboring cells. Scale bar, 1 μm. The genotypes of flies used are as follows and the number of flies used in (**a**) are indicated as follows (within parentheses): wild type – w^{1118} ($N=269$); mutant – *dYME1L*^{del} ($N=277$); Da-gal4 – *Da-gal4/+* ($N=115$); *dYME1L*^{del}, Da-gal4 – *dYME1L*^{del}*; Da-gal4/+* ($N=187$); *dYME1L*^{del}, Da>dYME1L or *dYME1L*^{del}, dYME1L – *dYME1L*^{del}*; Da-gal4/UAS-dYME1L-GFP* ($N=100$); *dYME1L*^{del}, Da>YME1L or *dYME1L*^{del}, YME1L – *dYME1L*^{del}*; Da-gal4/UAS-YME1L-GFP* ($N=79$)

(Figures 3a, b and e), the cristae of *dYME1L*^{del} mitochondria were misoriented (Figures 3c, d, f and g), giving rise to a 'patchy' appearance, and often loosely packed. Swollen mitochondria were also observed. In old *dYME1L*^{del} flies, cristae became more disorganized and there were many swollen mitochondria with much fewer cristae. In addition, old

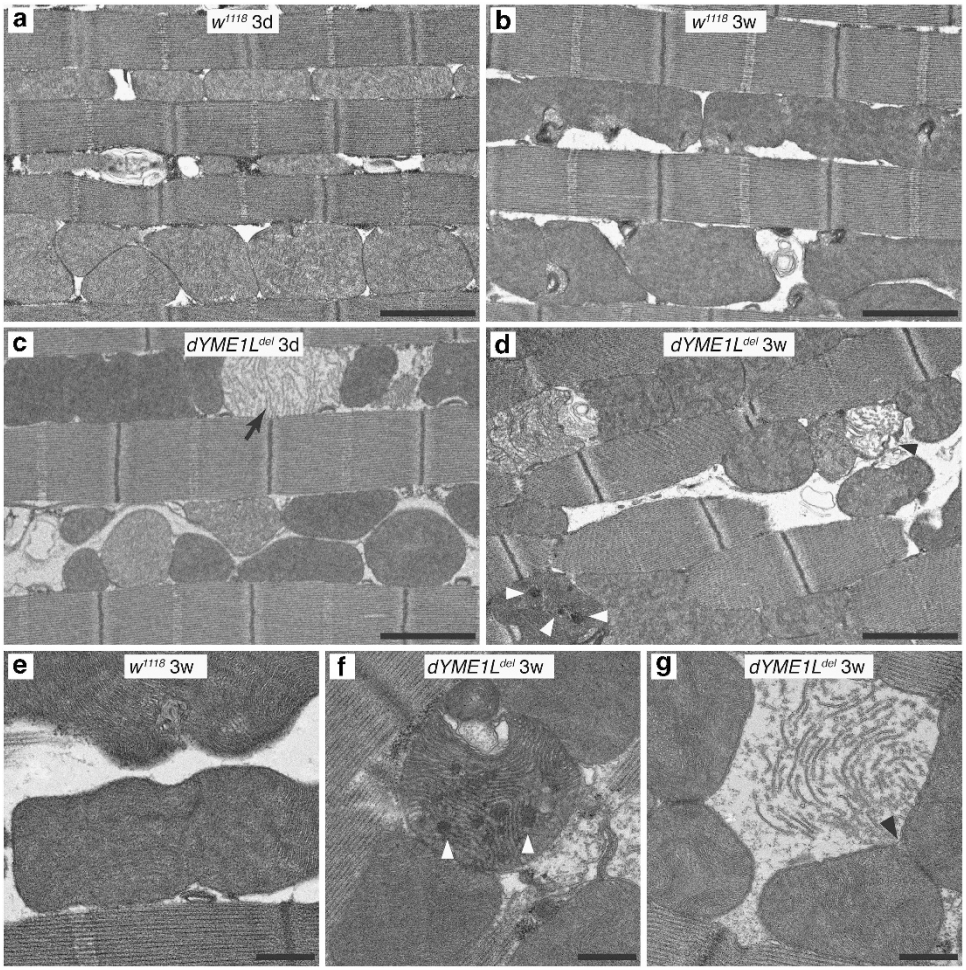

Figure 3 Mitochondrial anomalies in *dYME1L*^{del} flies. Electron micrographs of *w*^{1118} (**a**, **b** and **e**) and *dYME1L*^{del} (**c**, **d**, **f** and **g**) IFM. *w*^{1118}mitochondria display a relatively uniform morphology with densely packed arrays of cristae at both 3 days (3d) (**a**) and 3 weeks (3w) (**b** and **e**). By contrast, *dYME1L*^{del} mitochondria display various morphological anomalies, including reduced crista density (arrow in **c**) and disorganized cristae (**f** and **g**), and, in aged flies, dense aggregates (white arrowheads in **d** and **f**), swelling and membrane disruption (black arrowheads in **d** and **g**). Scale bar for (**a–d**), 2 μm and for (**e–j**), 0.5 μm

Figure 4 Muscle and photoreceptor cells of aged *dYME1L*^{del} flies undergo apoptotic cell death. (**a**) Confocal microscopic sections of IFM preparations from 4-week-old *w*^{1118} and *dYME1L*^{del} flies stained for cleaved caspase-3 (α-CC3, green), a marker of apoptotic cell death. Preparations are counterstained with DAPI (4',6-diamidino-2-phenylindole) to reveal nuclei (red) and phalloidin to reveal F-actin (blue). Scale bar, 10 μm. (**b**) Quantification of cleaved caspase-3-positive nuclei in wild-type and mutant IFM of aged flies ($N=5$). Eighty percent of nuclei display cleaved caspase-3 staining in aged mutant flies. Compared with wild-type flies, the number of apoptotic nuclei in *dYME1L*^{del} is significantly increased. Overexpressing ROS-scavenger proteins, such as SOD1 and SOD2, reduces cleaved caspase-3 staining, compared with the age-matched *dYME1L*^{del}, *Da-gal4* flies. Student's *t*-test is performed between the individual genetic manipulation and its corresponding control: *dYME1L*^{del} versus *w*^{1118}. *dYME1L*^{del}, *Da-gal4* versus *Da-gal4. dYME1L*^{del}, *Da-gal4, SOD1* versus *dYME1L*^{del}, *Da-gal4* and *dYME1L*^{del}, *Da-gal4, SOD2* versus *dYME1L*^{del}, *Da-gal4*. $^{*}P<0.05$, $^{**}P<0.01$ and $^{***}P<0.001$. (**c**) The model of the *Drosophila* apoptosis cascade used to inform the genetic suppression experiments in (**d**) and (**e**). (**d**) Restoring or suppressing photoreceptor cell loss in *dYME1L*^{del} flies by genetic manipulation. The number of photoreceptors per ommatidium ($N>100$) is assessed in 4-week-old flies ($N=5$) using the optical neutralization assay. Compared with the age-matched wild type, *dYME1L*^{del} flies show eye degeneration as evident by assessing ommatidium integrity. Overexpressing dYME1L, YME1L, P35, DIAP1, SOD1 and SOD2 or knocking down *dOmi*, *dArk* and *Dronc* rescues or suppresses the retinal degeneration in the mutant background. Student's *t*-test is performed. Analysis between wild type and mutant or gal4 only in the mutant background is indicated above the corresponding columns. Analysis between the individual genetic background and the corresponding genetic manipulation is indicated within the parentheses. $^{**}P<0.01$ and $^{***}P<0.001$. (**e**) Age-dependent locomotor impairment in *dYME1L*^{del} flies is suppressed either by knocking down *dArk*, *Dronc* and *dOmi* or overexpressing DIAP1. Student's *t*-test is performed. $^{*}P<0.05$ and $^{***}P<0.001$. Genotypes in (**b**) are as follows: wild type – *w*^{1118}; mutant – *dYME1L*^{del}. *Da-gal4-Da-gal4/+*. dYME1L^{del}; Da-gal4 – *dYME1L*^{del}*; Da-gal4/+*. dYME1L^{del}; SOD1 – *dYME1L*^{del}*, UAS-SOD1/dYME1L*^{del}*; Da-gal4/+*. dYME1L^{del}; SOD2 – *dYME1L*^{del}*, UAS-SOD2/dYME1L*^{del}*; Da-gal4/+*. In (**d**) and (**e**), wt-*Canton S.* GMR-P35-*gmr-P35; dYME1L*^{del}. GMR-DIAP1-*dYME1L*^{del}*; gmr-diap1*. Da-gal4-*dYME1L*^{del}*; Da-gal4/+*. dYME1L^{del}, Da > dYME1L-*dYME1L*^{del}*; Da-gal4/UAS-dYME1L-GFP*. dYME1L^{del}, Da > YME1L-*dYME1L*^{del}*; Da-gal4/UAS-YME1L-GFP*. dYME1L^{del}, Da > SOD1-*dYME1L*^{del}*, UAS-SOD1/dYME1L*^{del}*; Da-gal4/+*. dYME1L^{del}, Da > SOD2-*dYME1L*^{del}*, UAS-SOD2/dYME1L*^{del}*; Da-gal4/+*. dYME1L^{del}, Da > dArk^{IR}-*dYME1L*^{del}*; Da-gal4/UAS-dArk IR*. dYME1L^{del}, Da > Dronc^{IR}-*dYME1L*^{del}*; Da-gal4/UAS-Dronc IR*. dYME1L^{del}, Da > dOmi^{IR}-*dYME1L*^{del}*; Da-gal4/UAS-dOmi IR*

mutant flies had many electron-dense structures (Figures 3d and f) similar to the dense flocculant structures known to appear in mitochondria during aging and oxidative stress.[26]

Apoptosis underlies neurodegeneration in *dYME1L*^{del} flies. Mitochondrial dysfunction has been reported to trigger apoptosis in mammals.[27] However, mitochondrial involvement in apoptosis is still controversial in *Drosophila*.[28] The transmission electron microscopy of aged *dYME1L*^{del} flies displayed dying photoreceptor cells with apoptotic morphology, such as condensed nuclei, cell blebs and shrinkage, cytoplasmic condensation and losing cell–cell attachment (Figure 2d and Supplementary Figure S2a). Thus, we examined whether apoptotic cell death underlies the neuromuscular degeneration observed in *dYME1L*^{del} flies.

To confirm the existence of apoptosis, we used the cleaved caspase-3-specific antibody to stain the thoracic muscles for the activated Drice,[29–31] the *Drosophila* homolog of mammalian caspase-3, which resides in the cytosol as an inactive zymogen (procaspase-3) and translocates to the nucleus after proteolytic activation.[32] The cleaved caspase-3 staining was observed either associated or within >80% of the muscle nuclei of aged *dYME1L*^{del} flies, but could hardly be detected in either young *dYME1L*^{del} flies or wild-type flies (Figures 4a and b

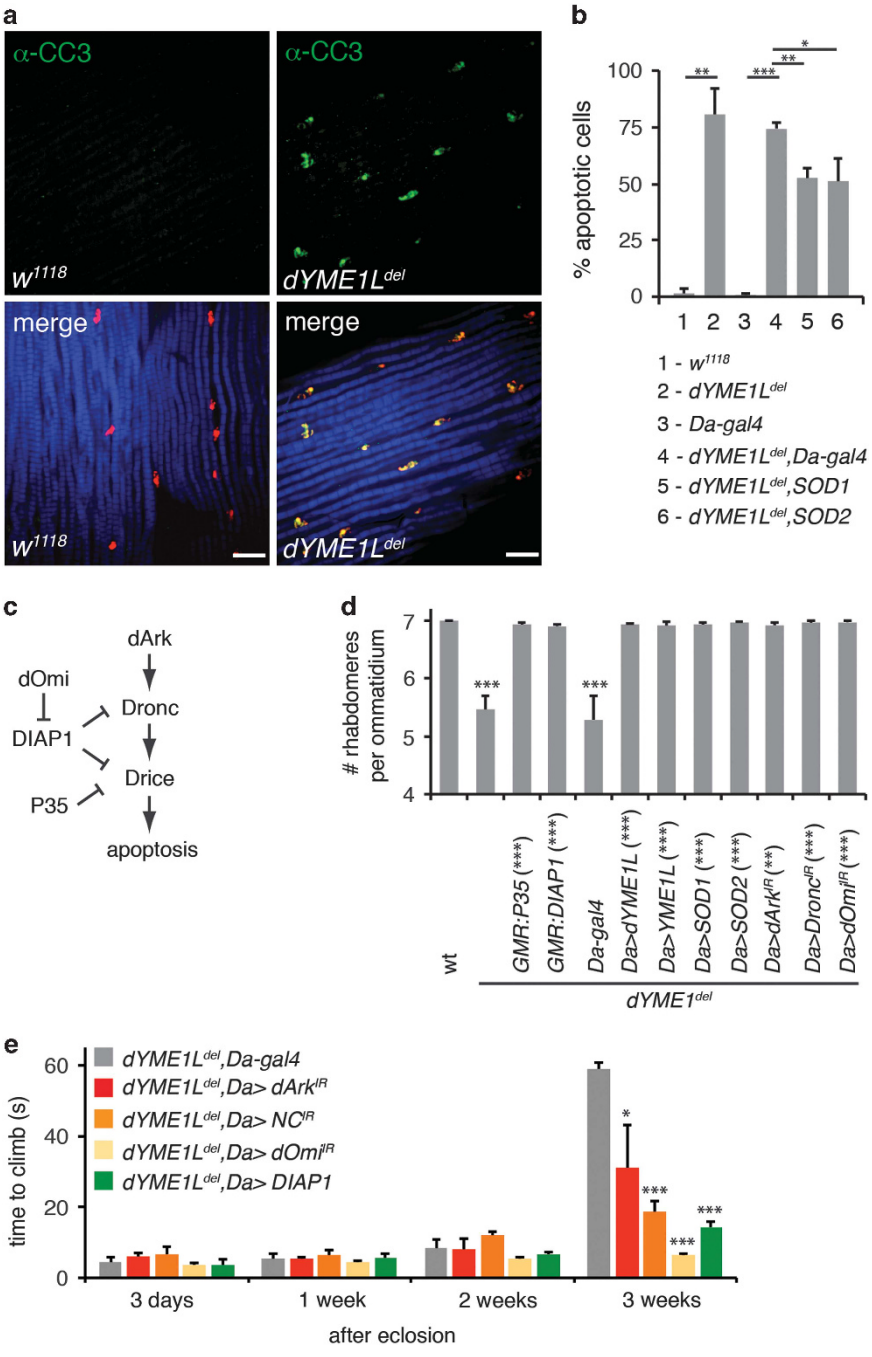

and Supplementary Figure S3a). Consistent with the positive cleaved caspase-3 staining, we also detected TUNEL-labeled nuclei in the muscle of aged *dYME1L*^{del} flies but not in the age-matched wild-type control (Supplementary Figure S3b). Meanwhile, we detected apoptosis in the photoreceptor cells of aged *dYME1L*^{del} flies using both cleaved caspase-3 antibody and cleaved Dcp-1 antibody [33] (Supplementary Figure S2b). These results demonstrate that the muscle and the retina of aged *dYME1L*^{del} flies undergo apoptosis.

To further explore whether apoptosis has causative roles in the degeneration, we overexpressed P35,[34–36] a baculovirus inhibitor for effector caspases, in the eye under the control of an eye-specific *gmr* promoter (*gmr-P35*). The overexpression of P35 suppressed the loss of photoreceptors in the ommatidia of *dYME1L*^{del} flies (Figure 4d and Supplementary Figure S2e). To test the involvement of the caspase cascade in the degeneration in *dYME1L*^{del} flies, we either overexpressed or knocked down the relevant genes (Figure 4c), and assessed the integrity of their ommatidia by the optical neutralization assay (Figure 4d and Supplementary Figures S2c and e). The effective *dArk* and *Dronc* knockdown suppressed the retinal degeneration, confirming that the dArk/Dronc cascade is indeed involved. In addition, both DIAP1 overexpression and the effective *dOmi* (*Drosophila* Htra2/Omi) knockdown also suppressed the retinal degeneration. Similarly, the age-dependent locomotor impairment in *dYME1L*^{del} flies was suppressed by blocking apoptosis upon DIAP1 overexpression or *dArk*, *Dronc* and *dOmi* knockdown (Figure 4e). Collectively, these results indicate that the mitochondrial i-AAA protease mutation leads to degeneration through dArk/Dronc-mediated apoptotic cascade.[37]

Elevated ROS level contributes to neurodegeneration in *dYME1L*^{del} flies. To determine whether the *dYME1L* mutation had any impact on the ETC, we analyzed the amount of various subunits of the ETC complexes by western blot (Figure 5a and Supplementary Figures S4a and b). Except for complex I, all the tested complexes were present in comparable amounts in wild-type flies and *dYME1L*^{del} flies, regardless of their ages. By contrast, the amount of complex I, as monitored by NDUFS3, one of its subunits, was markedly reduced in aged *dYME1L*^{del} flies compared with the age-matched wild-type flies, although it was normal in young *dYME1L*^{del} flies. Consistent with this observation, the activity of complex I (Figure 5b), but not the other complexes (Supplementary Figures S4c and d), was also reduced in the aged mutant flies.

Complex I is a major site of ROS production in the respiratory chain.[3] To test whether the impaired complex I leads to elevated ROS level in *dYME1L*^{del} flies, we used a colorimetric aconitase assay to indicate the status of oxidative damages in *dYME1L*^{del} flies (Figure 5c). Mitochondrial aconitase activity was indistinguishable between young wild-type flies and *dYME1L*^{del} flies. However, the aconitase activity was 20% lower in old *dYME1L*^{del} flies compared with that in the age-matched controls, indicating a higher amount of ROS in the mutant. To determine whether elevated ROS level contributes to the mutant phenotypes, we used the GAL4-UAS binary system to express ubiquitously the ROS-scavenging enzymes SOD1 and SOD2 in *dYME1L*^{del} flies under *Da-gal4* driver. Expression of these enzymes reduced the fraction of apoptotic nuclei, as indicated by the positive cleaved caspase-3 staining in the muscle of aged *dYME1L*^{del} flies (Figure 4b and Supplementary Figure S2c). Moreover, overexpression of SOD1 or SOD2 extended the lifespan of *dYME1L*^{del} flies moderately (Figure 5d), improved their locomotor activities (Figure 5f) and completely suppressed the photoreceptor neuron degeneration in the eye at the age of 4 weeks (Figure 4d and Supplementary Figure S3e). We also treated flies with *N*-acetyl cysteine (NAC), an antioxidant increasing the pool of reduced glutathione.[38] As NAC itself can extend lifespan,[39] we first titrated its dosage in wild-type flies (Supplementary Figure S4e). At a dose where no significant increase of lifespan was observed in wild type, the lifespan of *dYME1L*^{del} flies was slightly extended (Figure 5e). Taken together, these results demonstrate that mitochondrial i-AAA protease deficiency impairs complex I activity and leads to an increased level of ROS, which contributes to the degenerative phenotypes.

***dYME1L*^{del} flies display elevated mitochondrial unfolded protein stress and are more sensitive to environmental and genetic stresses.** Considering the proposed functions of i-AAA in mitochondrial proteostasis, we assessed the amount of HSP60, a marker for the unfolded protein response in mitochondria (UPR^{mt}).[40,41] Western blot analysis showed that HSP60 was more abundant in *dYME1L*^{del} flies compared with that in wild-type flies throughout adulthood (Figure 6a), supporting the idea that mitochondrial i-AAA protease deficiency disrupts mitochondrial protein homeostasis, leading to an elevated mitochondrial unfolded protein stress.

We also examined the levels of eIF2*α* and AKT phosphorylation that are considered as the downstream signal transducers of the matrix and IMS unfolded protein stresses,[42,43] respectively. We found that both eIF2*α* and AKT were hyperphosphorylated in *dYME1L*^{del} flies (Figure 6b), further confirming the elevated UPR^{mt}. However, eIF2*α* phosphorylation is also an indicator of ER unfolded protein response (UPR^{ER}). Indeed, BiP/GRP78, the master regulator of UPR^{ER} transduction pathway,[44–46] was upregulated in *dYME1L*^{del} flies throughout their adulthood (Supplementary Figure S5a). In addition, the general cellular protein turnover mechanisms, autophagy and ubiquitin–proteasome system, were both activated in the mutant flies (Figures 6c and d).

Elevated mitochondrial unfolded protein stress might render young *dYME1L*^{del} flies more susceptible compared with wild-type flies to protein stoichiometric disruption. To test this idea, we further challenged the mitochondrial protein homeostasis by overexpressing an endogenous mitochondrial protein, cytochrome *c* oxidase subunit IV (Cox4). Although overexpression of this protein had no obvious detrimental effects on wild-type flies, it led to complete mortality in *dYME1L*^{del} flies (Figure 6e). To test whether *dYME1L*^{del} flies were also more sensitive, compared with wild type, to oxidative stress, we treated them with paraquat, a known inducer of oxidative damages.[47] Paraquat treatment led to premature mortality in both wild-type flies and *dYME1L*^{del} flies, but *dYME1L*^{del} flies were much more sensitive to paraquat compared with wild-type flies (Figure 6f): it took only 3 days after paraquat treatment for half of the mutant flies to die. More than 50% of

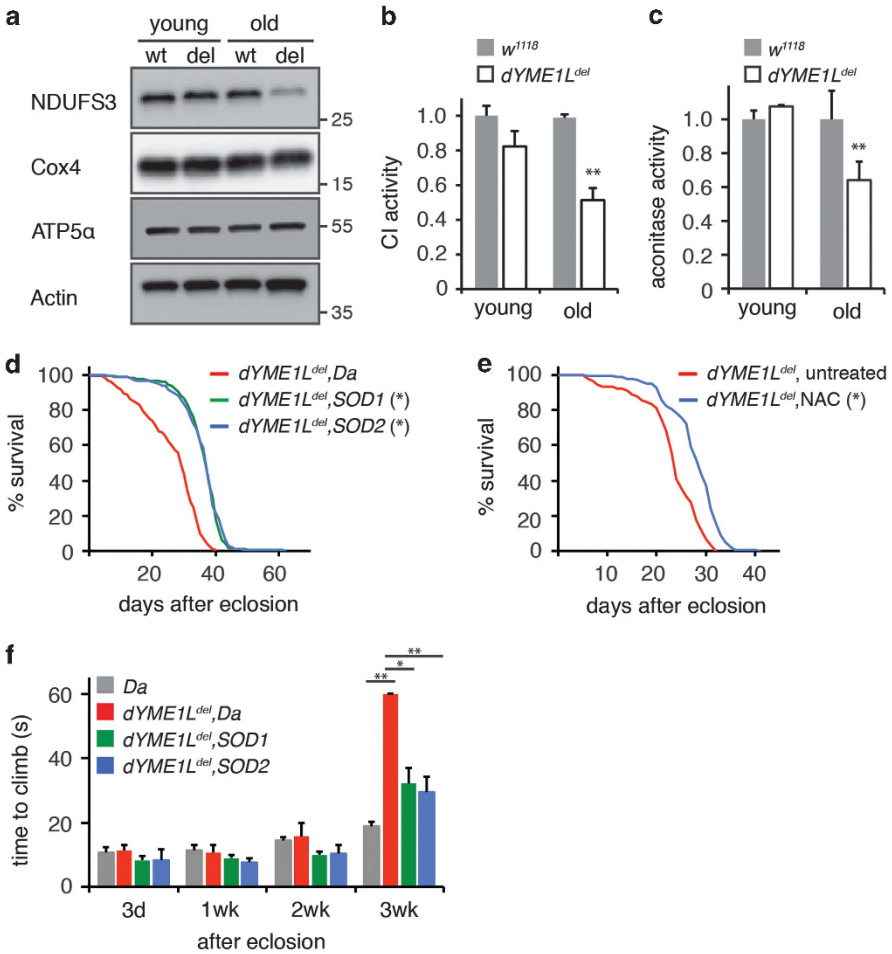

Figure 5 Complex I deficiency and elevated ROS in aged *dYME1L*^{del} flies. (**a**) Western blot analysis on whole-fly lysates reveals an age-dependent reduction in NDUFS3, a subunit of complex I in *dYME1L*^{del} flies. Subunits of complex IV (Cox4) and complex V (ATP5α) do not show such a pattern. (**b**) The complex I activity decreases with age in *dYME1L*^{del} flies. The isolated mitochondria from whole flies are tested. The activity is normalized to the young wild-type flies. CI, complex I. $^{**}P<0.01$ in Student's *t*-test. (**c**) *m*-Aconitase activity decreases with age in *dYME1L*^{del} flies. The activity is normalized to the age-matched wild-type flies. $^{**}P<0.01$ in Student's *t*-test. (**d**) Expression of ROS-scavenger proteins extends the lifespan of *dYME1L*^{del} flies. (**e**) NAC treatment also extends the lifespan of *dYME1L*^{del} flies ($N=149$) compared with the untreated control ($N=91$). The NAC dose used here, 1 μM, does not lead to lifespan extension in wild-type flies (Supplementary Figure S4e). Log-rank analysis is performed for (**d**) and (**e**). $^{*}P<0.0001$. (**f**) The climbing assay shows ROS-scavenger proteins significantly improve the locomotor activities of *dYME1L*^{del} flies. $^{*}P<0.05$ and $^{**}P<0.01$ in Student's *t*-test. The genotypes in (**a**)–(**c**) are as follows. wt – *w*^{1118}; del – *dYME1L*^{del}. Young: 3 days old; old: 3 weeks old. The genotypes in (**d**) and (**f**) and the number of flies used in (**d**) (within parentheses) are as follows. Da-*Da-gal4/+*. dYME1L^{del}, Da-*dYME1L*^{del}; *Da-gal4/+* ($N=115$); dYME1L^{del}, SOD1-*dYME1L*^{del}, *UAS-SOD1/dYME1L*^{del}; *Da-gal4/+* (N = 348); and dYME1L^{del}, SOD2-*dYME1L*^{del}, *UAS-SOD2/dYME1L*^{del}; *Da-gal4/+* ($N=308$)

the wild-type flies still survived 10 days after paraquat administration, but almost all of the *dYME1L*^{del} flies had died by that time. Taken together, these results suggest that the mitochondrial i-AAA protease mutation perturbs proteostasis inside mitochondria, and sensitizes them to genetic and environmental stresses.

Discussion

To understand the function of mitochondrial i-AAA protease in mitochondrial proteostasis and the degenerative mechanisms associated with mitochondrial AAA protease mutations, we generated a mitochondrial i-AAA protease mutant in *Drosophila*, thus creating the first YME1L-deficient animal model. We observed reduced complex I activities and consequently increased ROS levels in aged *dYME1L* mutant flies, which is consistent with studies on mammalian cultured cell lines.[16] Importantly, deletion of *dYME1L* caused an increase in mitochondrial unfolded protein stress and rendered mutant flies more susceptible to genetic and environmental stresses. Furthermore, it led to impaired locomotor activity and neural and muscular degeneration. These phenotypes are very similar to some key symptoms of human degenerative diseases associated with mutations in mitochondrial m-AAA proteases.[48] Notably, ectopic expression of human mitochondrial i-AAA protease, YME1L, rescued the degenerative phenotypes in the mutant flies, suggesting conserved physiological functions of mitochondrial i-AAA protease in metazoans.

In accordance with the intimate relationship between mitochondria and apoptosis in mammals, many mitochondrial mutations cause apoptotic myopathies and neuropathies.[49,50]

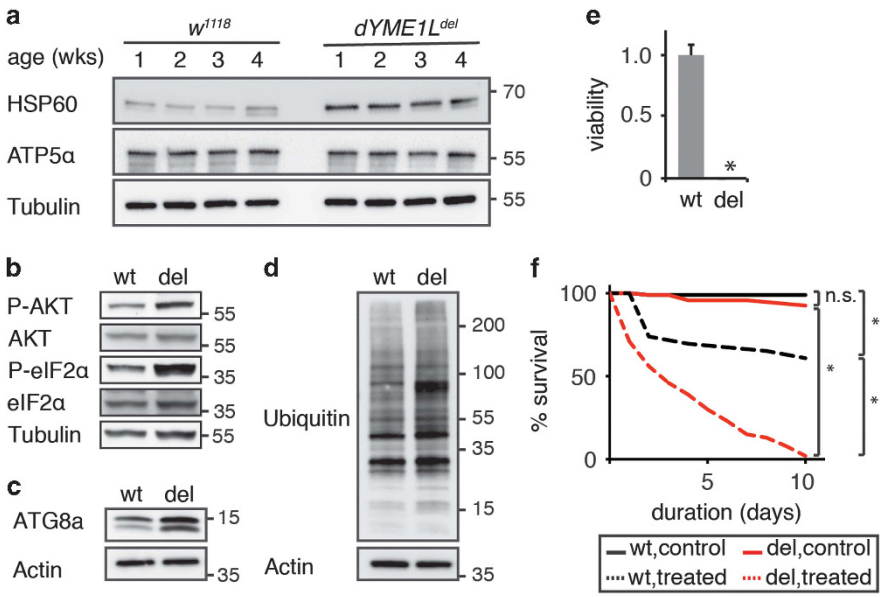

Figure 6 *dYME1L*^{del} flies are more vulnerable compared with wild-type flies to genetic and environmental stresses. (**a**) Western blot analysis on whole-fly lysates showing that the UPR^{mt}, as monitored by the HSP60 levels, is upregulated throughout the adulthood in *dYME1L*^{del} flies (1–4 weeks old after eclosion). (**b**) Western blot analysis on whole-fly lysates showing an elevated level of phospho-AKT (P-AKT) and, to a greater extent, of phospho-eIF2α (P-eIF2α), in 3-day-old *dYME1L*^{del} flies compared with the age-matched *w*^{1118}. (**c**) Western blot analysis on whole-fly lysates exhibiting the increase of ATG8a-II form in 3-day-old *dYME1L*^{del} flies compared with the age-matched *w*^{1118}. The ATG8a-I form is also increased. (**d**) Western blot analysis on whole-fly lysates displaying elevated level of conjugated ubiquitin in 3-day-old *dYME1L*^{del} flies compared with the age-matched *w*^{1118}. (**e**) Overexpressing the endogenous mitochondrial protein Cox4 in the *dYME1L*^{del} background leads to complete lethality (*). The ectopic expression is driven by *tub-gal4*. (**f**) Paraquat treatment leads to quicker mortality in *dYME1L*^{del} compared with that in wild-type flies. Log-rank analysis is performed. *$P < 0.0001$; n.s., not significant. wt in (**b**)–(**e**) and (**f**) are *w*^{1118} and *dYME1L*^{del}/+, respectively. del: *dYME1L*^{del}

Several common neurodegenerative diseases such as Parkinson's disease and Huntington's disease are also associated with mitochondrion-dependent apoptosis.[51] However, mitochondrial involvement in apoptosis in *Drosophila* remains uncertain.[52,53] Particularly, the cytochrome *c* involvement in the apoptosome activation is highly debatable.[28] Instead of being a direct 'activator', mitochondria are considered as the docking sites to receive death signals and release proapoptotic molecules. In *Drosophila*, the Apaf-1-related protein dArk is associated with and constitutively activates the initiator caspase Dronc, which in turn activates the effector caspase Drice. dArk/Dronc cascade is involved in the apoptosis of aged *dYME1L*^{del} flies as knockdown of either of them suppresses the degenerative phenotypes. DIAP1 inhibits both Dronc and Drice and thereby suppresses the apoptosis. DIAP1 can be degraded by the transcriptional upregulation of H99 cluster (RHG) genes, namely *reaper*, *hid* and *grim*.[37] However, we did not detect any significant transcriptional upregulation of these genes in aged *dYME1L*^{del} flies (Supplementary Figure S6). DIAP1 can also be degraded by dOmi, a mitochondrial serine protease in the IMS, when released into the cytoplasm.[54] Actually *dOmi* knockdown suppresses the degenerative phenotypes, namely retinal degeneration and locomotor impairment, in aged *dYME1L*^{del} flies (Figures 4d and e and Supplementary Figure S2e).

In addition, we found the dOmi upregulation at both transcriptional level and protein level (Supplementary Figures S5b and c), and the ruptured mitochondria in the electron microscopic images of the IFM from *dYME1L*^{del} flies (Figures 3d and g). Given that ectopic overexpression of dOmi in *Drosophila* developing eyes causes cell death,[20,54] these results suggest that dOmi might be released through mitochondrial breakages in *dYME1L*^{del} flies to trigger the apoptotic cascade (Supplementary Figure S7). Of note, dOmi protein level was also markedly increased in the old flies, regardless of their genotypes (Supplementary Figure S5c). The lack of cell death in old wild-type files argues that, although necessary, the increase of the endogenous dOmi alone might not be sufficient to trigger apoptosis. In yeast, the mitochondrial i-AAA protease is also required for the turnover of Ups1 and Ups2, which regulate the accumulation of cardiolipin (CL) and phosphatidylethanolamine, respectively.[55] Thus, impaired phospholipid metabolism might be another inroad leading to the membrane remodeling, rupture and eventually apoptosis in mitochondrial i-AAA protease mutant flies (Supplementary Figure S7). Our results not only support that mitochondrial disruption *per se* could trigger apoptosis in *Drosophila* but also suggest that apoptotic neuronal death might be a common degenerative mechanism associated with mitochondrial AAA protease mutations.

i-AAA is required for maintaining stoichiometry of all the ETC complexes encoded by both the nuclear and the mitochondrial genomes. Why *dYME1L*^{del} specifically impairs complex I in aged flies remains to be explored. Probably, complex I is the largest ETC complex and consists of more than 40 different subunits, which may render it particularly vulnerable. Indeed many mitochondrial mutations perturbing mitochondrial proteostasis compromise complex I.[41,56] Flies carrying the *Drosophila Sicily* mutation that disrupts complex I assembly also display reduced complex I activity, elevated ROS level and retinal degeneration.[56] However, there is no detectable apoptosis in the *Sicily* mutant, suggesting the

existence of caspase-independent cell death and the insufficiency for ROS alone to elicit apoptosis. We found that the expression of ROS-scavenger proteins suppressed the retinal degeneration and extended the lifespan of *dYME1L*^{del} flies. Further, we showed in proof of principle that the antioxidant NAC was also able to extend the lifespan of *dYME1L*^{del} flies. Thus, ROS may act synergistically with other mitochondrial deficiencies to trigger or promote apoptosis in *dYME1L*^{del} flies (Supplementary Figure S7). More importantly, our work resonates with a recent study showing that NAC treatment rescued mitochondrial defects in cultured AFG3L2-depleted mouse neurons,[57] and suggests that manipulating ROS level could be a potential disease-curbing strategy.

In mammals, OPA1, a substrate of i-AAA, controls crista remodeling and mediates apoptotic neurodegeneration.[58,59] However, the S2 cleavage site of i-AAA is not present in *Drosophila* OPA1.[60] Ectopic overexpression of another mitochondrial protease, Rhomboid-7, could process dOPA1.[61] Our western blot analysis revealed similar patterns of dOPA1 isoforms in wild-type and mutant flies (Supplementary Figure S5d), further substantiating that dYME1L is unlikely to be required for OPA1 processing. On the other hand, although the eIF2*α* phosphorylation attenuated protein translation, all the OPA1 isoforms appeared to be more abundant in the *dYME1L*^{del} background compared with that in the wild-type background, suggesting a role of i-AAA protease in removing excessive IMS proteins. Nonetheless, it is still possible that other substrates of i-AAA could regulate crista remodeling in *Drosophila* as OPA1 in mammals.

In *dYME1L*^{del} flies, sustained UPR^{ER} and general protein turnover mechanisms are observed. Thus, it would be interesting to dissect how a mitochondrial stress triggers UPR^{ER} and understand the pathophysiological significance of their interplay.

Materials and Methods

Molecular biology. *Drosophila* genes *CG3499-PB* (*dyme1l-PB*), *CG7654* (*tom20*), *CG10664* (*cox4*) and *CG8479-PA* (*dOpa1-PA*) were cloned from embryonic cDNA library. The human mitochondrial i-AAA protease subunit gene, *yme1l*, was cloned from cDNA clone MGC: 3533 IMAGE: 3637576 (NIH-MGC Project, Gaithurberg, MD, USA). Tags, such as GFP, mCherry and myc, were fused at the C terminus of the individual mitochondrial proteins. The genes were cloned into pAW and pPW vectors.

Cell culture. *Drosophila* S2 cells were cultured in Schneider's *Drosophila* medium (Invitrogen, Carlsbad, CA, USA) supplemented with 10% FBS. Cellfectin II (Invitrogen) was used as the vehicle to deliver plasmids into cells. Before confocal fluorescence images were taken, cells were seeded in concanavalin A-pretreated coverglass chambers.

***Drosophila* genetics.** Fly stocks and all genetic crosses were maintained at 25 °C on standard cornmeal agar media under a 12:12 light-dark cycle. The fly stocks, BL14902 (P-element insertion in *CG3499* gene region), BL5782 (*gmr-diap1*), BL5774 (*gmr-P35*), BL28544 (*dOmi* RNAi) and BL32963 (*Dronc* RNAi), were obtained from Bloomington Stock Center (Bloomington, IN, USA). *dArk* RNAi line was generously provided by Pascal Meier (London, UK) through NIG and MITILS.[62] *UAS-SOD1* and *UAS-SOD2* were kindly provided by John Phillips (Guelph, Ontario, CA, USA). Gal4 driver lines, *tub-gal4* and *Da-gal4*, were kept in the lab. Transgenic flies, *UAS-dYME1L-GFP*, *UAS-YME1L-GFP*, *UAS-Cox4-GFP* and *UAS-dOPA1-myc*, were made by BestGene embryonic injection service. w^{1118} was used as a wild-type control, and experiments were carried out on male flies, unless otherwise indicated. Fly age was counted as days per weeks after eclosion.

We generated CG3499-deletion line by imprecise excision of the P-element insertion line BL14902, $y^1;CG3499^{KG01861}/CyO;ry^{506}$. P-element excision was screened in the *CG3499* gene region by PCR analysis on the extracted genomic DNA using two primers that amplify the *CG3499* gene region (left primer: 5′-CGATAGGGACTCTTTGTCTATCCT-3′; right primer: 5′-ACATAGGTTGCA GTAGTCTGGTCAC-3′). In wild-type and in precise excision lines, these primers amplify a 3.6 kb fragment. Smaller PCR products indicate imprecise excisions. The PCR products were sequenced to identify imprecise excisions removing large portions of the *CG3499* gene region (left primer: 5′-ACTGTACGGAGAGG CAGTTTAGAT-3′; right primer: 5′-GGTTCGATTAACGGAGTAGTAGTGC-3′). One imprecise excision line removing 2 kb *CG3499*-genomic region including the majority of the exons was recovered and named *dYME1L*^{del}.

Immunohistochemistry. *Drosophila* tissues were dissected in 4% PFA PBS and permeablized in 4% PFA PBST (0.1% Triton X-100 in PBS) for 30 min. The samples were washed with PBST and blocked in 5% FBS, 0.5% BSA PBST (blocking buffer) for 1 h and then incubated with primary antibodies overnight at 4 °C. Phalloidin (Alexa Fluor; Life Technologies, Eugene, OR, USA; 1 : 40) was used to highlight F-actin, whereas the cleaved caspase-3 antibody (9661; Cell Signaling; 1 : 400) or the cleaved Dcp-1 antibody (9578; Cell Signaling; 1 : 100) was used to detect apoptosis. After extensive washing with the blocking buffer, the samples were treated with secondary antibodies (Alexa Fluor; Life Technologies; 1 : 200) in the blocking buffer for 45 min. After extensive washes, samples were placed in VECTASHIELD Mounting Medium with DAPI (Vector Lab, Berlingame, CA, USA) before confocal imaging. For the TUNEL assay, Click-iT TUNEL Alexa Fluor Imaging Assay Kit (Life Technologies) was used following the manufacturer's protocol.

Confocal microscopic image acquisition. Images were acquired using an UltraVIEW VoX spinning disk confocal imaging system (Perkin-Elmer, Waltham, MA, USA) on the AxioObserver.Z1 inverted microscope (Zeiss, Thornwood, NY, USA) equipped with a ×63 objective lens (numerical aperture: 1.4; immersion medium: oil) and cameras (Hamamatsu C9100-13 and C10600-10B (ORCA-R2, Bridgewater, NJ, USA)). Live cells with transient transfection were imaged in Schneider's *Drosophila* medium supplemented with 10% FBS. Fixed tissues were imaged in VECTASHIELD Mounting Medium with DAPI. Imaging processing was performed using Volocity (Perkin-Elmer). Brightness and contrast were adjusted but no nonlinear adjustment (gamma settings) was allowed.

Longevity assay. Male flies were collected and maintained at 25 °C with a transfer for fresh food every 2–3 days. The number of dead flies was recorded on a daily basis. The survival rate was calculated by the percentage of total flies surviving.

Behavior assays. To avoid the impact of CO_2 anesthesia, flies were grouped into individual vials (10 per vial, 3 vials per age for the climbing assay) or were individually placed into a vial (10 flies per age for the bang sensitivity test) one day before the test. In the climbing test, the 10 flies were transferred into a long glass tube by tapping down from the original vials. The tube was gently tapped down on the bench top to send the flies to the bottom of the tube. The flies were allowed to climb up the tube and the time that took them to reach a predefined height was measured. If it took more than 60 s for the flies to reach the desired height, the time was arbitrarily scored 60 s. Three groups of 10 flies for each individual genotype at a desired age (three biological replicates) were tested. In the bang sensitivity test, flies were transferred into an empty vial individually by tapping down from the original vials. The vial was then vortexed (maximal setting) for 10 s to paralyze the fly temporarily. The time for each fly to recover (right itself and resume normal behavior) was recorded. Any trial in which the fly remained stunned for more than 60 s was terminated and recorded as 60 s. Ten flies were individually tested for each genotype and age. The age-matched w^{1118}, *da-gal4/+* and *dYME1L*^{del}*; da-gal4/+* flies were used as control for *dYME1L*^{del} flies, *dYME1L*^{del}*; da-gal4/+* flies and *dYME1L*^{del}*; da-gal4/UAS construct* flies, respectively. Experiments on the flies at the same age after eclosion were performed at the same time, to minimize variability contributed by environmental factors.

Viability assay. The crosses between predefined genotypes were performed and the expected ratio of different genotypes in the progeny was calculated. Seven days later, the parental flies were removed. When the progeny eclosed, the number of individual genotypes were counted for 10 days. The real ratio was calculated.

The viability was expressed as the percentage of the real ratio to the expected ratio. Three individual experiments were set up for each cross.

Immunobloting. Whole flies were collected and homogenized in RIPA buffer supplemented with protease inhibitors, Complete Mini Protease inhibitor cocktail tablets (Roche, Penzberg, Germany), and phosphatase inhibitors, PhosSTOP EASYpack (Roche). Total protein was assayed by the BCA method (Thermo Scientific, Rockford, IL, USA). Equal amount of total protein was subjected to Tris-glycine SDS-PAGE and subsequently transferred to PVDF membrane. The membrane was blocked by 5% non-fat milk TBST (0.1% Tween-20 in TBS) or SuperBlock blocking buffer (Thermo Scientific). Specific antibodies were used to detect NDUFS3 (17D95; Abcam, Cambridge, MA, USA), Cox4 (ab16056; Abcam), ATP5α (15H4C4; Abcam), actin (C4; Millipore, Billerica, MA, USA), HSP60 (D307; Cell Signaling), phospho-*Drosophila* AKT (Ser505) (4054; Cell Signaling), AKT (9272; Cell Signaling), eIF2α (ab26197; Abcam), phospho-eIF2α (ab32157; Abcam), β-tubulin (E7; Hybridoma Bank, Iowa City, IA, USA), ubiquitin (3933; Cell Signaling), BiP (PAB2462; Abnova, Iowa City, IA, USA), dOmi (Emad Alnemri, Philadelphia, PA, USA)[63] and ATG8a (Gabor Juhasz, Budapest, Hungary).[64] We used myc antibody (9E10; Hybridoma Bank) to detect the overexpression of myc-tagged dOPA1 (dOPA1-myc). HRP-conjugated anti-mouse Ig and anti-rabbit IgG secondary antibodies were used (GE Healthcare, Pittsburgh, PA, USA). Super-Signal West Pico or Dura Chemiluminescent Substrate (Thermo Scientific) was used as a developer and ImageQuant LAS4000 (GE) was used for imaging. Densitometry quantification was performed using the 1D gel analysis function of ImageQuant TL software (GE).

Mitochondrial isolation and complex activity assay. Mitochondria were isolated following a published protocol.[56] Briefly, whole flies were homogenized in mitochondrial isolation buffer (5 mM HEPES, 210 mM D-mannitol, 70 mM sucrose and 1 mM EGTA). The lysate was subjected to centrifugation at 3000 × *g* for 10 min at 4 °C. The supernatant was decanted to a new microcentrifuge tube and centrifuged at 8000 × *g* for 20 min at 4 °C. The supernatant (cytoplasmic fraction) was discarded and the pellet was resuspended and washed with mitochondrial isolation buffer. The resuspension was again subjected to centrifugation at 8000 × *g* for 20 min at 4 °C. The supernatant was discarded and the mitochondrion-enriched pellet was suspended in the assay buffer (250 mM sucrose, 2 mM EDTA and 100 mM Tris-HCl, pH 7.4).

Complex I activity was assayed in a spectrophotometer at 340 nm in a reaction mixture of 25 mM potassium phosphate, pH 7.5, 0.2 mM NADH and 1.7 mM potassium ferricyanide. Complex II plus III (succinate-cytochrome *c* oxidoreductase) activity was assayed at 550 nm in a reaction mixture of 25 mM potassium phosphate, pH 7.5, 2 mM potassium cyanide, 80 μM cytochrome *c* and 5 mM succinate.[65] Complex IV (cytochrome *c* oxidase, COX) activity was assayed in 10 mM potassium phosphate and 25 μM reduced cytochrome *c*.[66] The enzymatic kinetics was measured with the SWIFT II Wavescan software (GE healthcare) and the slope (velocity) was recorded. All the activities were normalized to total protein assayed. Then, all the samples were further normalized to the samples of the young wild-type flies (3 days old).

Aconitase assay. Mitochondrial aconitase activity of the whole flies was assayed with a Colorimetric Kit (Sigma, St. Louis, MO, USA) according to the manufacturer's instructions (MAK051; Sigma). Biological triplicates were assayed per genotype per age. All the activities were normalized to total protein assayed. All samples were then normalized to the age-matched wild-type flies.

Analysis of retinal degeneration. Male flies of predefined genotypes were reared at 25 °C under a 12:12 light-dark cycle. Flies were killed at different ages (5 per group) and the heads were cut off before counting the mean number of rhabdomeres per ommatidium using the optical neutralization technique.[67] White-eyed flies were crossed with *Canton S* to make the genotypes to test in a red-eyed background. Data for each individual fly was based on examination of more than 100 ommatidia.

Transmission electron microscopy. Tissues were dissected out in fixative (2.5% glutaraldehyde, 1% PFA, 0.12 M sodium cacodylate buffer, pH 7.4, with the addition of 0.1% dishwashing detergent). Then, they were collected into microporous specimen capsules and fixed in the fixation buffer. The samples were held in a fixative without a detergent overnight at 4 °C. The muscles were postfixed in 1% OsO_4, *en bloc* stained with 1% uranyl acetate, dehydrated in an ethanol series, embedded in Embed 812 resin (Electron Microscopy Sciences, Hatfield, PA, USA) and cured at 60 °C for 2 days. Sections were stained with uranyl acetate and lead citrate and examined with a JEM 1400 electron microscope (JEOL, Pleasanton, CA, USA) equipped with an AMT XR-111 digital camera (Advanced Microscopy Techniques, Wobrun, MA, USA).

Paraquat resistance test. We used *dYME1L*^{del} flies as mutant flies and *dYME1L*^{del}/+ flies as the wild-type (control) flies. Flies (100 flies per group) were starved for 6 h in vials supplemented with only filter paper soaked with 5% sucrose solution. Later, the flies were transferred to vials with only filter paper soaked with 10 mM paraquat in 5% sucrose solution or filter paper soaked with 5% sucrose solution overnight. Then, flies were transferred to fresh vials. Survival was determined on a daily basis for the subsequent 10 days.

NAC treatment. To test whether NAC could improve the lifespan of *dYME1L*^{del} flies, we first titrated the dosage on wild-type flies. A drop of NAC solution (50 μl) with different concentrations (0, 1, 10 and 100 μM) was dropped on the fresh food a day before these vials were used to replace the old vials. Longevity assay was performed on *dYME1L*^{del} flies treated with 1 μM NAC.

Transcriptional level analysis. Total RNA from *Drosophila* tissues was isolated using TRIzol reagent (Ambion, Carlsbad, CA, USA). The isolated RNA was treated with RQ1 RNase-free DNase (Promega, Madison, WI, USA) at 37 °C for 15 min. Then, the treated RNA was cleaned up using RNeasy Mini Kit (Qiagen, Valencia, CA, USA). RevertAid First Strand cDNA Synthesis Kit (Thermo Scientific) was used for first-strand synthesis. One-step quantitative real-time PCR was performed on 7900HT Fast Real-Time PCR system by using SYBR GreenER qPCR SuperMix (Life Technologies).

dOmi (*CG8464*) was detected by dOmi set (forward primer dOmi-RT-L: 5′-TCG GCACGGACAAGATTACG-3′; reverse primer dOmi-RT-R: 5′-ACGGCTTCAAT GGTGTTGGG-3′). *dArk* (*CG6829*) was detected by dArk set (forward primer dArk-RT-L: 5′-TTTGAAGAAGCCCATAAACAAGTG-3′; reverse primer dArk-RT-R: 5′-TGGAAACGACCGTGGTTAGTAA-3′). *Dronc* (*CG8091*) was detected by Dronc set (forward primer NC-RT-L: 5′-TACCGAGTGTTTCGTAATGG-3′; reverse primer NC-RT-R: 5′-GGAAATGGTCCTTGATCTTC-3′). *Reaper* (*CG4319*) was detected by Reaper set (forward primer Reaper-RT-L: 5′-AGCAGAAGGAGCAGCAGATC-3′; reverse primer Reaper-RT-R: 5′-ATGGCTTGCGATATTTGCCG-3′). *Hid* (*CG5123*) was detected by Hid set (forward primer Hid-RT-L: 5′-TCATCTTCGTCCTCCGCATC; reverse primer Hid-RT-R: 5′-CGTGAAATTGCAAGAGGGGC). *Grim* (*CG4345*) was detected by Grim set (forward primer Grim-RT-L: 5′-CCAAGGACAACTGCA ACAGC-3′; reverse primer Grim-RT-R: 5′-CGCTGCTGATCTCGAAGGAT-3′). *β-actin* (forward primer actin-RT-L: 5′-GCCCATCTACGAGGGTTATGC-3′; reverse primer actin-RT-R: 5′-CAAATCGCGACCAGCCAG-3′) or *rp49* (forward primer rp49-RT-L: 5′-GCAAGCCCAAGGGTATCGA-3′; reverse primer rp49-RT-R: 5′-TAACCGATGTTG GGCATCAG-3′) was set up as the internal control. Expression levels of the individual genes were normalized to the level of the internal control.

Statistics. The data was shown as the mean ± S.D. of at least three independent experiments unless specified differently. Significance of differences was calculated by the two-tailed *Student's t*-test using the *T* Test function provided by Microsoft Excel. For the survival and lifespan experiments, log-rank analysis was performed by virtue of the built-in function of survival in GraphPad Prism 6 (La Jolla, CA, USA).

Conflict of Interest

The authors declare no conflict of interest.

Acknowledgements. We thank F Chanut and Y Chen for comments on the manuscript; P Connelly and C Brantner at NHLBI EM Core for technical assistance; J Phillips, P Meier, the TRiP at Harvard Medical School, National Institute of Genetics and Mitsubishi Kagaku Institute of Life Sciences, and Bloomington stock center for fly stocks; X Zhu for *Drosophila* embryonic cDNA library; E Alnemri, G Juhasz and Hybridoma Bank for antibodies; BestGene for embryonic injection service. This work was supported by NHLBI intramural program.

1. Beal MF. Mitochondria take center stage in aging and neurodegeneration. *Ann Neurol* 2005; **58**: 495–505.

2. Calvo SE, Mootha VK. The mitochondrial proteome and human disease. *Annu Rev Genom Hum Genet* 2010; **11**: 25–44.
3. Rigoulet M, Yoboue ED, Devin A. Mitochondrial ROS generation and its regulation: mechanisms involved in H(2)O(2) signaling. *Antioxid Redox Signal* 2011; **14**: 459–468.
4. Voos W. Chaperone-protease networks in mitochondrial protein homeostasis. *Biochim Biophys Acta* 2013; **1833**: 388–399.
5. Arnold I, Langer T. Membrane protein degradation by AAA proteases in mitochondria. *Biochim Biophys Acta* 2002; **1592**: 89–96.
6. Leonhard K, Herrmann JM, Stuart RA, Mannhaupt G, Neupert W, Langer T. AAA proteases with catalytic sites on opposite membrane surfaces comprise a proteolytic system for the ATP-dependent degradation of inner membrane proteins in mitochondria. *EMBO J* 1996; **15**: 4218–4229.
7. Leonhard K, Guiard B, Pellecchia G, Tzagoloff A, Neupert W, Langer T. Membrane protein degradation by AAA proteases in mitochondria: extraction of substrates from either membrane surface. *Mol Cell* 2000; **5**: 629–638.
8. Casari G, De Fusco M, Ciarmatori S, Zeviani M, Mora M, Fernandez P *et al.* Spastic paraplegia and OXPHOS impairment caused by mutations in paraplegin, a nuclear-encoded mitochondrial metalloprotease. *Cell* 1998; **93**: 973–983.
9. Di Bella D, Lazzaro F, Brusco A, Plumari M, Battaglia G, Pastore A *et al.* Mutations in the mitochondrial protease gene AFG3L2 cause dominant hereditary ataxia SCA28. *Nat Genet* 2010; **42**: 313–321.
10. Pierson TM, Adams D, Bonn F, Martinelli P, Cherukuri PF, Teer JK *et al.* Whole-exome sequencing identifies homozygous AFG3L2 mutations in a spastic ataxia-neuropathy syndrome linked to mitochondrial m-AAA proteases. *PLoS Genet* 2011; **7**: e1002325.
11. Tatsuta T, Langer T. Quality control of mitochondria: protection against neurodegeneration and ageing. *EMBO J* 2008; **27**: 306–314.
12. Anand R, Wai T, Baker MJ, Kladt N, Schauss AC, Rugarli E *et al.* The i-AAA protease YME1L and OMA1 cleave OPA1 to balance mitochondrial fusion and fission. *J Cell Biol* 2014; **204**: 919–929.
13. Mishra P, Carelli V, Manfredi G, Chan DC. Proteolytic Cleavage of Opa1 Stimulates Mitochondrial Inner Membrane Fusion and Couples Fusion to Oxidative Phosphorylation. *Cell Metab* 2014; **19**: 630–641.
14. Ruan Y, Li H, Zhang K, Jian F, Tang J, Song Z. Loss of Yme1L perturbates mitochondrial dynamics. *Cell Death Dis* 2013; **4**: e896.
15. Song Z, Chen H, Fiket M, Alexander C, Chan DC. OPA1 processing controls mitochondrial fusion and is regulated by mRNA splicing, membrane potential, and Yme1L. *J Cell Biol* 2007; **178**: 749–755.
16. Stiburek L, Cesnekova J, Kostkova O, Fornuskova D, Vinsova K, Wenchich L *et al.* YME1L controls the accumulation of respiratory chain subunits and is required for apoptotic resistance, cristae morphogenesis, and cell proliferation. *Mol Biol Cell* 2012; **23**: 1010–1023.
17. Pandey UB, Nichols CD. Human disease models in Drosophila melanogaster and the role of the fly in therapeutic drug discovery. *Pharmacol Rev* 2011; **63**: 411–436.
18. Clark IE, Dodson MW, Jiang CG, Cao JH, Huh JR, Seol JH *et al. Drosophila* pink1 is required for mitochondrial function and interacts genetically with parkin. *Nature* 2006; **441**: 1162–1166.
19. Greene JC, Whitworth AJ, Kuo I, Andrews LA, Feany MB, Pallanck LJ. Mitochondrial pathology and apoptotic muscle degeneration in Drosophila parkin mutants. *Proc Natl Acad Sci USA* 2003; **100**: 4078–4083.
20. Park J, Lee SB, Lee S, Kim Y, Song S, Kim S *et al.* Mitochondrial dysfunction in Drosophila PINK1 mutants is complemented by parkin. *Nature* 2006; **441**: 1157–1161.
21. Juhola MK, Shah ZH, Grivell LA, Jacobs HT. The mitochondrial inner membrane AAA metalloprotease family in metazoans. *FEBS Lett* 2000; **481**: 91–95.
22. Nussleinvolhard C, Lohsschardin M, Sander K, Cremer C. Dorso-ventral shift of embryonic primordia in a new maternal-effect mutant of Drosophila. *Nature* 1980; **283**: 474–476.
23. Schupbach T, Wieschaus E. Germline autonomy of maternal-effect mutations altering the embryonic body pattern of Drosophila. *Dev Biol* 1986; **113**: 443–448.
24. Nussleinvolhard C, Frohnhofer HG, Lehmann R. Determination of anteroposterior polarity in *Drosophila*. *Science* 1987; **238**: 1675–1681.
25. Jackson GR. Guide to understanding *Drosophila* models of neurodegenerative diseases. *PLoS Biol* 2008; **6**: e53.
26. Cole NB, Daniels MP, Levine RL, Kim G. Oxidative stress causes reversible changes in mitochondrial permeability and structure. *Exp Gerontol* 2010; **45**: 596–602.
27. Wang XD. The expanding role of mitochondria in apoptosis. *Gene Dev* 2001; **15**: 2922–2933.
28. Mollereau B. Cell death: what can we learn from flies? Editorial for the special review issue on *Drosophila* apoptosis. *Apoptosis* 2009; **14**: 929–934.
29. Srinivasan A, Roth KA, Sayers RO, Shindler KS, Wong AN, Fritz LC *et al. In situ* immunodetection of activated caspase-3 in apoptotic neurons in the developing nervous system. *Cell Death Differ* 1998; **5**: 1004–1016.
30. Muro I, Berry DL, Huh JR, Chen CH, Huang HX, Yoo SJ *et al.* The Drosophila caspase Ice is important for many apoptotic cell deaths and for spermatid individualization, a nonapoptotic process. *Development* 2006; **133**: 3305–3315.
31. Fan Y, Bergmann A. The cleaved-caspase-3 antibody is a marker of caspase-9-like DRONC activity in Drosophila. *Cell Death Differ* 2010; **17**: 534–539.
32. Kamada S, Kikkawa U, Tsujimoto Y, Hunter T. Nuclear translocation of caspase-3 is dependent on its proteolytic activation and recognition of a substrate-like protein(s). *J Biol Chem* 2005; **280**: 857–860.
33. Querenet M, Goubard V, Chatelain G, Davoust N, Mollereau B. Spen is required for pigment cell survival during pupal development in *Drosophila*. *Dev Biol* 2015; **402**: 208–215.
34. Hay BA, Wolff T, Rubin GM. Expression of baculovirus P35 prevents cell death in *Drosophila*. *Development* 1994; **120**: 2121–2129.
35. Martin DN, Baehrecke EH. Caspases function in autophagic programmed cell death in *Drosophila*. *Development* 2004; **131**: 275–284.
36. Davidson FF, Steller H. Blocking apoptosis prevents blindness in *Drosophila* retinal degeneration mutants. *Nature* 1998; **391**: 587–591.
37. Steller H. Regulation of apoptosis in Drosophila. *Cell Death Differ* 2008; **15**: 1132–1138.
38. Kelly GS. Clinical applications of *N*-acetylcysteine. *Altern Med Rev* 1998; **3**: 114–127.
39. Brack C, Bechter-Thuring E, Labuhn M. *N*-acetylcysteine slows down ageing and increases the life span of *Drosophila melanogaster*. *Cell Mol Life Sci* 1997; **53**: 960–966.
40. Broadley SA, Hartl FU. Mitochondrial stress signaling: a pathway unfolds. *Trends Cell Biol* 2008; **18**: 1–4.
41. Pimenta de Castro I, Costa AC, Lam D, Tufi R, Fedele V, Moisoi N *et al.* Genetic analysis of mitochondrial protein misfolding in *Drosophila melanogaster*. *Cell Death Differ* 2012; **19**: 1308–1316.
42. Pellegrino MW, Nargund AM, Haynes CM. Signaling the mitochondrial unfolded protein response. *BBA Mol Cell Res* 2013; **1833**: 410–416.
43. Jovaisaite V, Mouchiroud L, Auwerx J. The mitochondrial unfolded protein response, a conserved stress response pathway with implications in health and disease. *J Exp Biol* 2014; **217**: 137–143.
44. Ryoo HD, Steller H. Unfolded protein response in *Drosophila* – why another model can make it fly. *Cell Cycle* 2007; **6**: 830–835.
45. Hoozemans JJM, Veerhuis R, Van Haastert ES, Rozemuller JM, Baas F, Eikelenboom P *et al.* The unfolded protein response is activated in Alzheimer's disease. *Acta Neuropathol* 2005; **110**: 165–172.
46. Fouillet A, Levet C, Virgone A, Robin M, Dourlen P, Rieusset J *et al.* ER stress inhibits neuronal death by promoting autophagy. *Autophagy* 2012; **8**: 915–926.
47. McCarthy S, Somayajulu M, Sikorska M, Borowy-Borowski H, Pandey S. Paraquat induces oxidative stress and neuronal cell death; neuroprotection by water-soluble Coenzyme Q10. *Toxicol Appl Pharmacol* 2004; **201**: 21–31.
48. Atorino L, Silvestri L, Koppen M, Cassina L, Ballabio A, Marconi R *et al.* Loss of m-AAA protease in mitochondria causes complex I deficiency and increased sensitivity to oxidative stress in hereditary spastic paraplegia. *J Cell Biol* 2003; **163**: 777–787.
49. DiMauro S. Pathogenesis and treatment of mitochondrial myopathies: recent advances. *Acta Myol* 2010; **29**: 333–338.
50. Pareyson D, Piscosquito G, Moroni I, Salsano E, Zeviani M. Peripheral neuropathy in mitochondrial disorders. *Lancet Neurol* 2013; **12**: 1011–1024.
51. Mattson MP. Apoptosis in neurodegenerative disorders. *Nat Rev Mol Cell Bio* 2000; **1**: 120–129.
52. Abdelwahid E, Rolland S, Teng X, Conradt B, Hardwick JM, White K. Mitochondrial involvement in cell death of non-mammalian eukaryotes. *Biochim Biophys Acta* 2011; **1813**: 597–607.
53. Hay BA, Guo M. Caspase-dependent cell death in *Drosophila*. *Annu Rev Cell Dev Biol* 2006; **22**: 623–650.
54. Challa M, Malladi S, Pellock BJ, Dresnek D, Varadarajan S, Yin YW *et al.* Drosophila Omi, a mitochondrial-localized IAP antagonist and proapoptotic serine protease. *EMBO J* 2007; **26**: 3144–3156.
55. Potting C, Wilmes C, Engmann T, Osman C, Langer T. Regulation of mitochondrial phospholipids by Ups1/PRELI-like proteins depends on proteolysis and Mdm35. *EMBO J* 2010; **29**: 2888–2898.
56. Zhang K, Li ZH, Jaiswal M, Bayat V, Xiong B, Sandoval H *et al.* The C8ORF38 homologue Sicily is a cytosolic chaperone for a mitochondrial complex I subunit. *J Cell Biol* 2013; **200**: 807–820.
57. Kondadi AK, Wang S, Montagner S, Kladt N, Korwitz A, Martinelli P *et al.* Loss of the m-AAA protease subunit AFG3L2 causes mitochondrial transport defects and tau hyperphosphorylation. *EMBO J* 2014; **33**: 1011–1026.
58. Frezza C, Cipolat S, de Brito OM, Micaroni M, Beznoussenko GV, Rudka T *et al.* OPA1 controls apoptotic cristae remodeling independently from mitochondrial fusion. *Cell* 2006; **126**: 177–189.
59. Ramonet D, Perier C, Recasens A, Dehay B, Bove J, Costa V *et al.* Optic atrophy 1 mediates mitochondria remodeling and dopaminergic neurodegeneration linked to complex I deficiency. *Cell Death Differ* 2013; **20**: 77–85.
60. Olichon A, ElAchouri G, Baricault L, Delettre C, Belenguer P, Lenaers G. OPA1 alternate splicing uncouples an evolutionary conserved function in mitochondrial fusion from a vertebrate restricted function in apoptosis. *Cell Death Differ* 2007; **14**: 682–692.
61. Rahman M, Kylsten P. Rhomboid-7 over-expression results in Opa1-like processing and malfunctioning mitochondria. *Biochem Biophys Res Commun* 2011; **414**: 315–320.

62. Leulier F, Ribeiro PS, Palmer E, Tenev T, Takahashi K, Robertson D *et al.* Systematic in vivo RNAi analysis of putative components of the *Drosophila* cell death machinery. *Cell Death Differ* 2006; **13**: 1663–1674.
63. Khan FS, Fujioka M, Datta P, Fernandes-Alnemri T, Jaynes JB, Alnemri ES. The interaction of DIAP1 with dOmi/HtrA2 regulates cell death in *Drosophila*. *Cell Death Differ* 2008; **15**: 1073–1083.
64. Takats S, Nagy P, Varga A, Pircs K, Karpati M, Varga K *et al*. Autophagosomal Syntaxin17-dependent lysosomal degradation maintains neuronal function in *Drosophila*. *J Cell Biol* 2013; **201**: 531–539.
65. Chen Z, Qi Y, French S, Zhang G, Garcia RC, Balaban R *et al.* Genetic mosaic analysis of a deleterious mitochondrial DNA mutation in *Drosophila* reveals novel aspects of mitochondrial regulation and function. *Mol Biol Cell* 2015; **26**: 674–684.
66. Hill JH, Chen Z, Xu H. Selective propagation of functional mitochondrial DNA during oogenesis restricts the transmission of a deleterious mitochondrial variant. *Nat Genet* 2014; **46**: 389–392.
67. Xu H, Lee SJ, Suzuki E, Dugan KD, Stoddard A, Li HS *et al*. A lysosomal tetraspanin associated with retinal degeneration identified via a genome-wide screen. *EMBO J* 2004; **23**: 811–822.

Supplementary Information accompanies this paper on Cell Death and Differentiation website (http://www.nature.com/cdd)